



Beijing Institute of Applied Physics and
Computational Mathematics (IAPCM)

Comparative study of blast loading on solid and porous structures

—— Zababakhin Scientific Talks (2025) ——

Supervisor: *Jun Chen*

Reporter: *JiaRui Li*

2025.05.20



Contents

- **Background**
- **Objective**
- **Methodology**
- **Numerical setup**
- **Results and Analysis**
- **Discussion**
- **Conclusion**

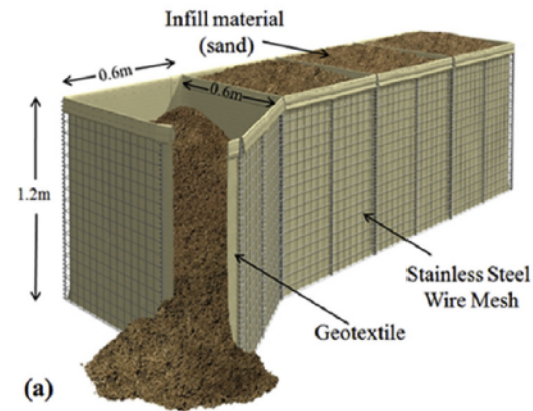
Background: Blast loading and mitigation

- **Blast loading generated by the detonation of high explosives poses a serious threat to nearby individuals and structures**
- **Porous media (granular materials, aqueous foams) vs. concrete walls: superior blast mitigation performance with reduced costs**



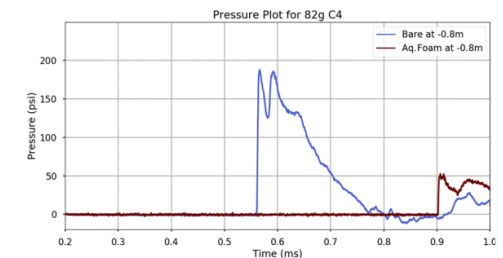
Strong blast wave ahead of fireball from a homogeneous C-4 detonation

D.L. Frost, *Shock Waves* (2018)



Military fortifications using granular materials (sand)

P. Vivek, *Geotextiles and Geomembranes* (2017)

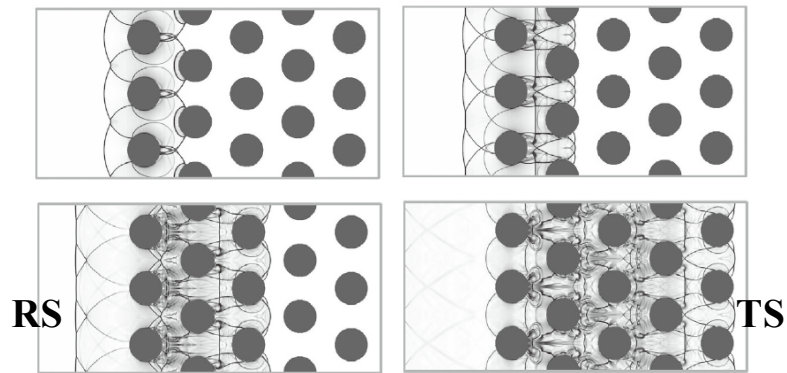


Mitigated overpressure from a C4 blast immersed in dry aqueous foam

K. Ahmed, *AIP advances* (2020)

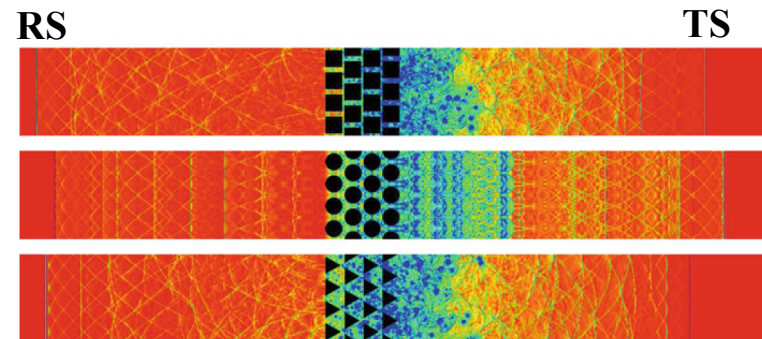
Background: Complex shock-particle interactions

- The evolution of blast load (measured by pressure) at the shock-impacted interface attracts most attention
- The complex interactions between blast/shock wave and porous media influence the interface load



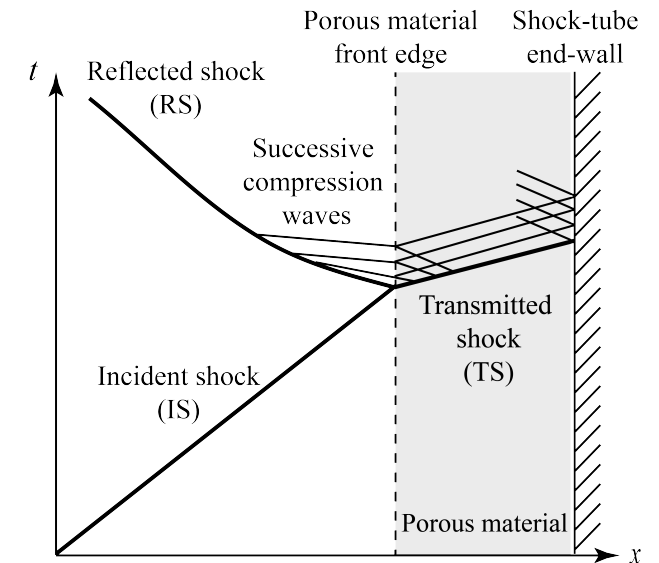
Reflection and transmission when a planar shock impacts a regular cylinder array

T. Ogawa, *Computers and Fluids* (2013)



The formation and propagation of reflected/transmitted shock waves when a planar shock impacts porous media with different geometrical shapes

A. Chaudhuri, *Shock Waves* (2013)

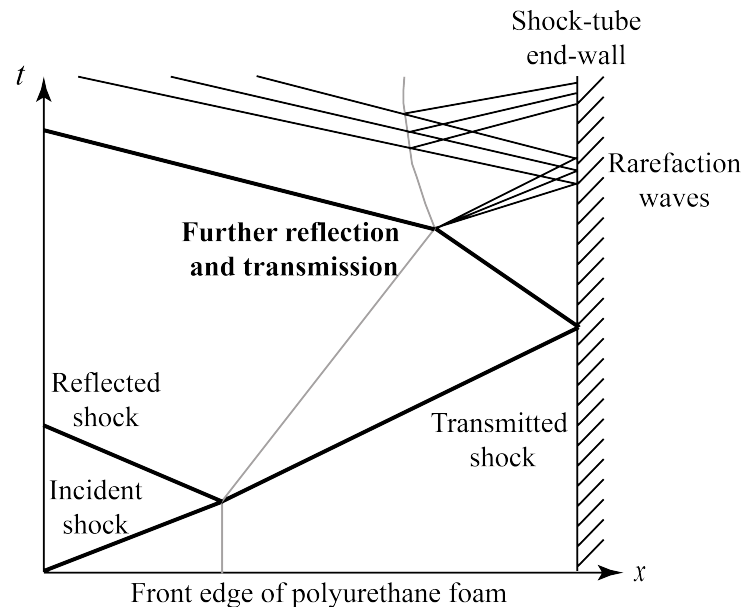


A well accepted (x, t) diagram of various waves involved in shock-particle interactions

A. Levy, *Experiments in Fluids* (1993)

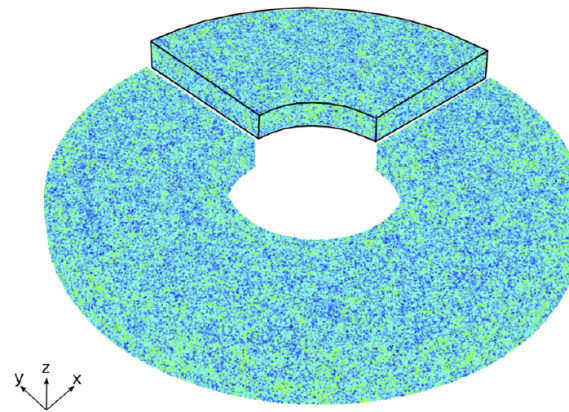
Background: Explosion in confined space

- In a confined explosion scenario, shock waves may experience multiple reflections at the boundaries
- Cannot be simplified as a single shock impact on structures



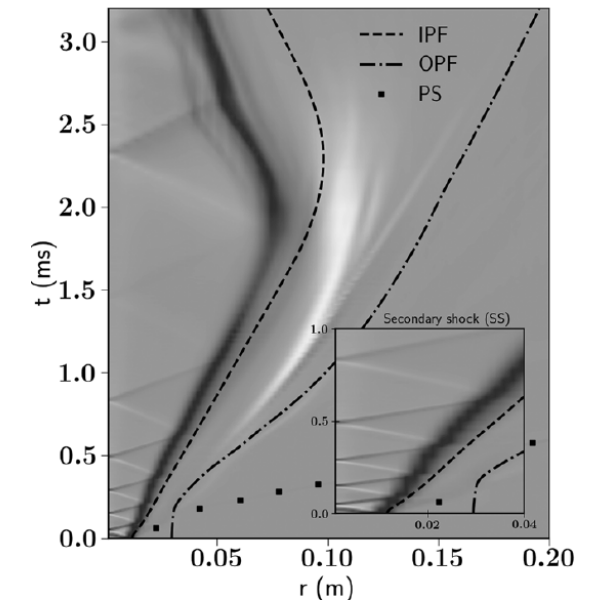
(x, t) diagram of various waves when a flexible foam near the end-wall impacted by a planar shock

B.W. Skews, *Shock Wave Propagation in Porous Media* (1992)



A particle ring under central explosion, showing reciprocating shock waves between the shock-particle interface and the center of configuration

R.B. Koneru, *Physics of Fluids* (2020)



Background: Current state of research

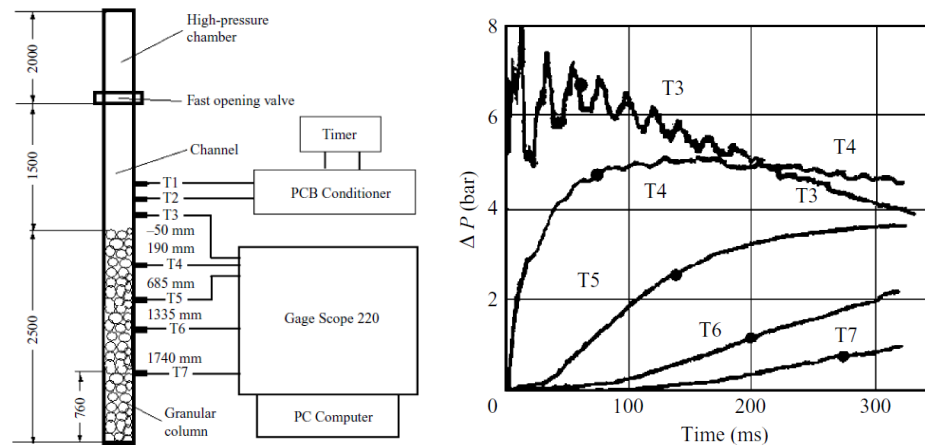
➤ Experimental: Shock tube set-ups

- Load evolution ← mounted pressure transducers
- The propagation of various waves ← schlieren imaging

The relationship among interface load, wave evolution, and multiple parameters remains unclear

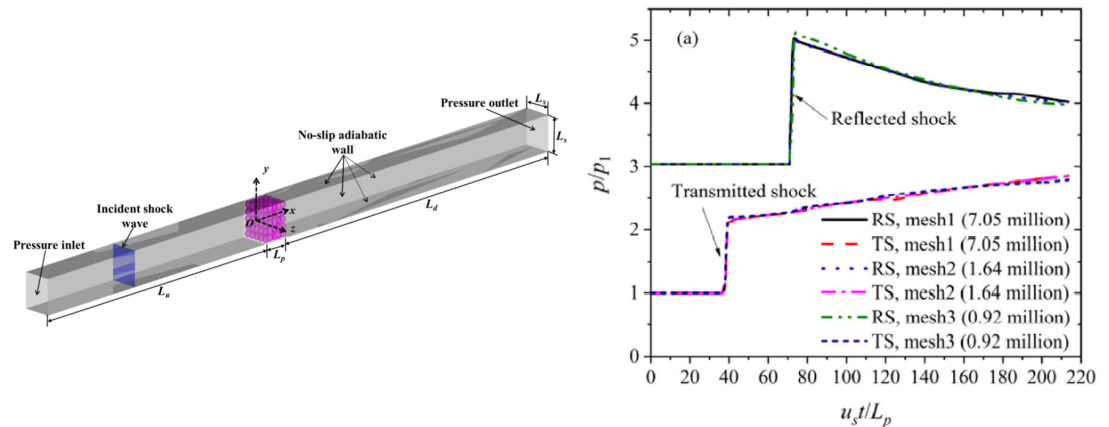
➤ Numerical: Multiphase flow approaches for shock-particle interactions

Limited research on load evolution under multiple shock loading



Schematic drawing of the shock tube set-up and the pressure traces recorded by the transducers

A. Britan, *Journal of Fluid Mechanics* (2007)



Simulation of the interaction between a single planar shock and a movable particle curtain, with the pressure profiles upstream and downstream of the curtain

L.T. Zhang, *Powder Technology* (2023)

Objectives

➤ Our focus

Scenarios involving multiple shock waves generated by explosions in confined space

➤ Our goals

- Investigate **the characteristics of interface load and the underlying mechanisms governing its evolution**
- Explore how **different load conditions and porous media properties** influence the evolution of interface load

Methodology: Introduction of CMP-PIC

➤ Compressible Multiphase Particle-in-cell method (CMP-PIC)

A coarse-grained Euler-Lagrange approach B.L. Tian, *Journal of Computational Physics* (2020)

• Gas phase: Volume-averaged Eulerian equations

$$\frac{\partial(\varepsilon \rho_f)}{\partial t} + \nabla \cdot (\varepsilon \rho_f \mathbf{u}_f) = 0$$

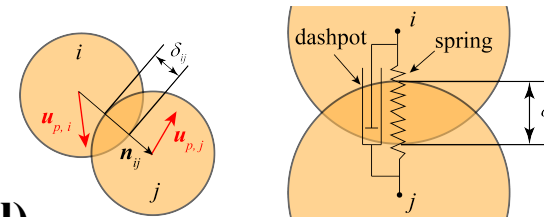
$$\frac{\partial(\varepsilon \rho_f \mathbf{u}_f)}{\partial t} + \nabla \cdot (\varepsilon \rho_f \mathbf{u}_f \mathbf{u}_f) + \nabla(\varepsilon P_f) = P_f \nabla \varepsilon + \sum_i \left[\phi_{p,i} \rho_{p,i} D_{p,i} (\mathbf{u}_{p,i} - \bar{\mathbf{u}}_f) \right]$$

**Coupling term:
the particle drag force
and the associated work**

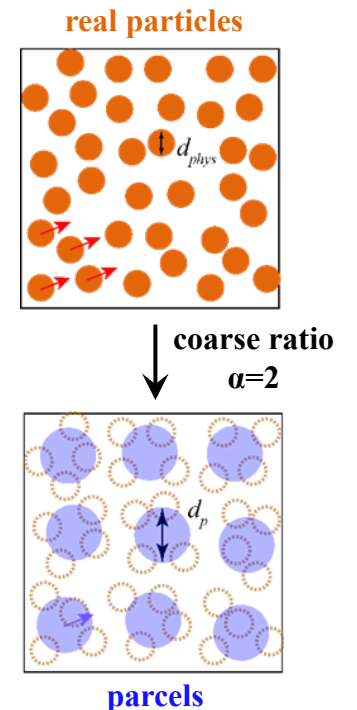
$$\frac{\partial(\varepsilon \rho_f E_f)}{\partial t} + \nabla \cdot (\varepsilon \rho_f E_f \mathbf{u}_f + \varepsilon P_f \mathbf{u}_f) = P_f \nabla \varepsilon \cdot \bar{\mathbf{u}}_p + \sum_i \left[\phi_{p,i} \rho_{p,i} D_{p,i} (\mathbf{u}_{p,i} - \bar{\mathbf{u}}_f) \cdot \mathbf{u}_{p,i} \right]$$

• Particle phase: Newton's 2nd law

$$\frac{d\mathbf{u}_{p,i}}{dt} = \underbrace{D_{p,i} (\mathbf{u}_{p,i} - \bar{\mathbf{u}}_f)}_{\text{Drag force (Di Felice model)}} - \underbrace{\frac{\nabla P_f}{\rho_{p,i}}}_{\text{Pressure gradient force}} + \underbrace{\frac{1}{m_{p,i}} \sum_j \mathbf{F}_{C,ij}}_{\text{Collision force (Soft sphere model)}}$$



P.A. Cundall, *Géotechnique* (2008)



The basic unit of the particle phase is the coarse-grained parcel **8**

Methodology: CMP-PIC

➤ Numerical method for solving fluid equations

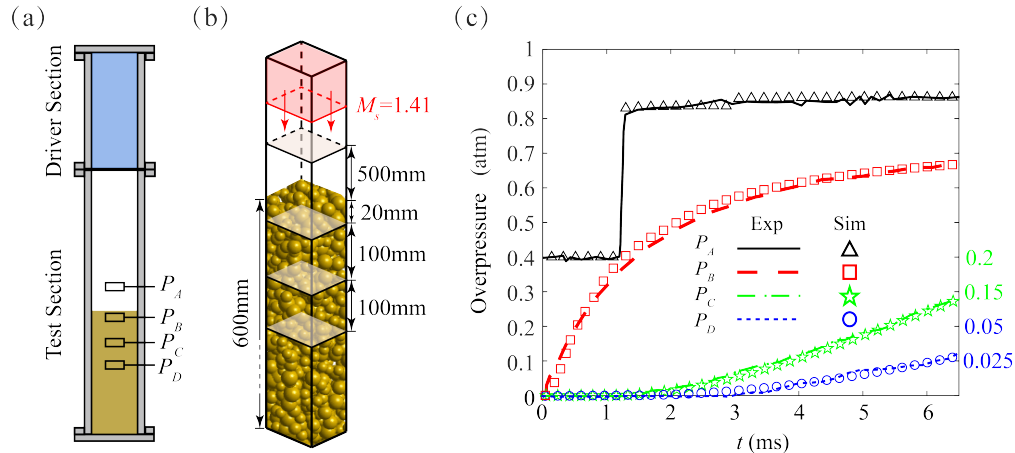
- Time integration ← third-order Runge-Kutta scheme
- Spatial discretization of convective terms ← fifth-order WENO
- Spatial discretization of flux and non-conservative terms ← HLL/HLLC scheme with Riemann solvers

➤ Advantages

- Complete governing equations for the gas phase, **enabling non-isothermal processes**
- A four-way coupling strategy **capable of simulating complex shock-particle interactions**
- Coarse-grained approach **suitable for computing laboratory-scale system**
- Capability to represent grain-scale heterogeneities

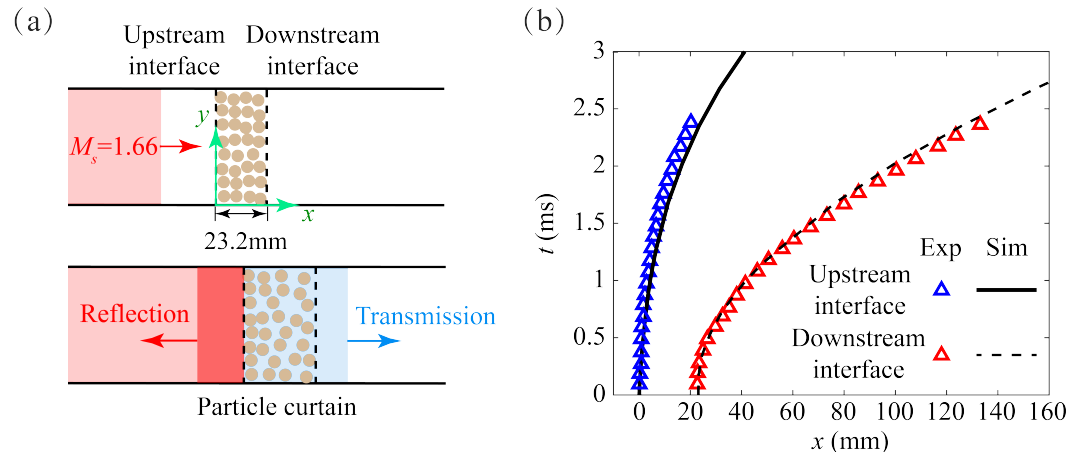
Methodology: Validation tests

➤ Test : Particle column impacted by shock wave



The simulated pressure histories showed good consistency with those of the experiment

➤ Test : Particle column impacted by shock wave

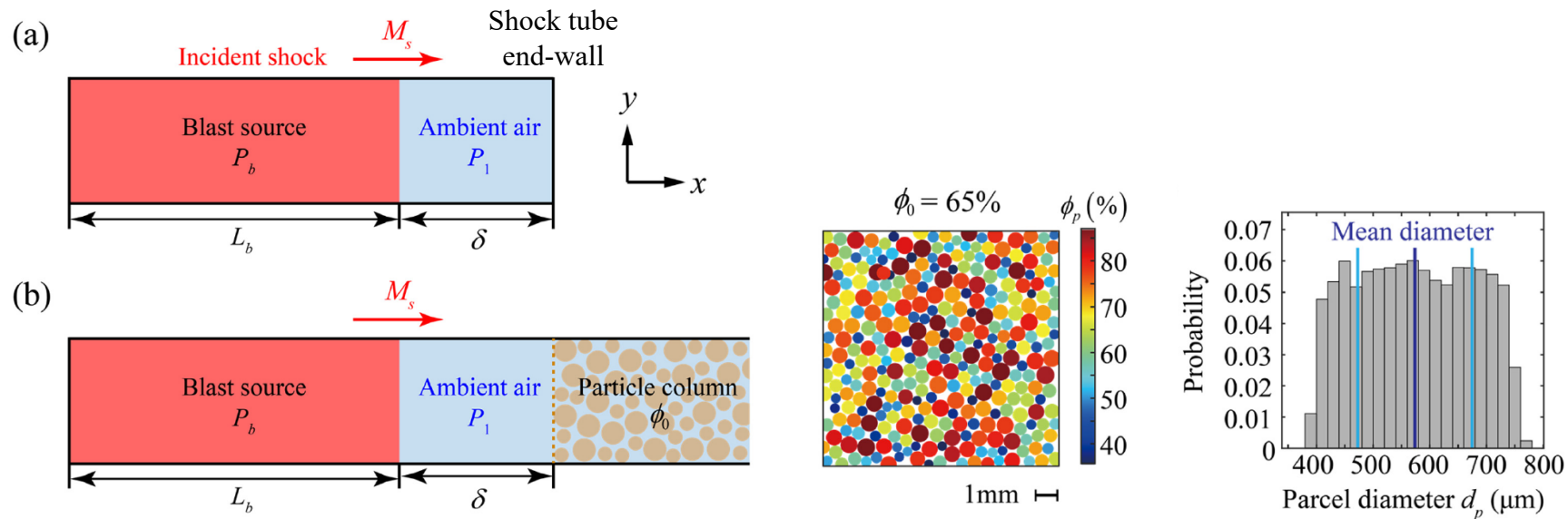


The trajectories of upstream and downstream interface closely matched those obtained in the experiment

CMP-PIC approach can correctly handle problems involving complex shock-particle interactions

Numerical setup

- Similar to the widely employed shock tube set-ups
 - 2-dimensional simulation
 - Blast source ← high-pressure gas
 - Simulation of explosions in confined spaces
 - Strong planar shock impact **a solid wall or a dense particle column**



Numerical setup

➤ Investigated parameters

- Blast energy**

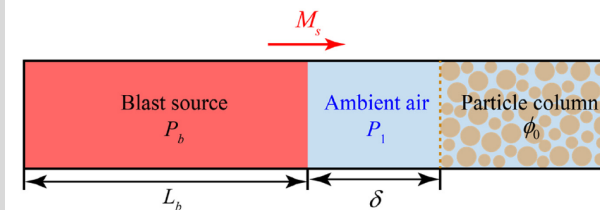
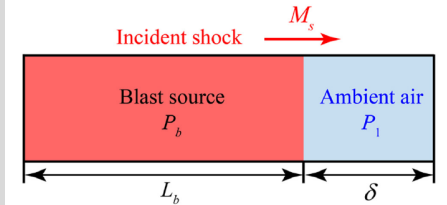
Blast energy depends on the blast pressure and length of the driver section

- Stand-off distance**

Initial solid volume fraction

- Particle column properties**

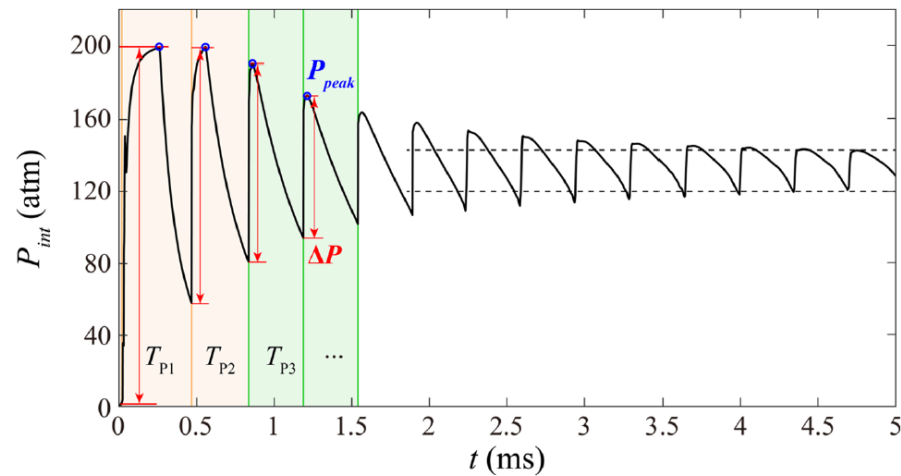
Case name	M_s	E_b (kJ)	P_b (atm)	L_b (mm)	δ (mm)	L_b/δ	ϕ_0	k (10^{-12} m^2)	Particle motion
W1	2.61	283.7	200	40	20	2	...	Permeability	...
W2	2.19	85.1	60	40	20	2
W3	1.56	12.2	8.6	40	20	2
W4	2.61	1134.8	200	160	20	8
W5	2.61	283.7	200	40	80	0.5
P1	2.61	283.7	200	40	20	2	0.65	6.77	No
P2	2.19	85.1	60	40	20	2	0.65	6.77	No
P3	1.56	12.2	8.6	40	20	2	0.65	6.77	No
P4	2.61	1134.8	200	160	20	8	0.65	6.77	No
P5	2.61	283.7	200	40	80	0.5	0.65	6.77	No
P6	2.61	283.7	200	40	20	2	0.5	33.33	No
P7	2.61	283.7	200	40	20	2	0.4	90.00	No
P8	2.19	85.1	60	40	20	2	0.65	6.77	Yes



Results: Blast loading on **solid** interface

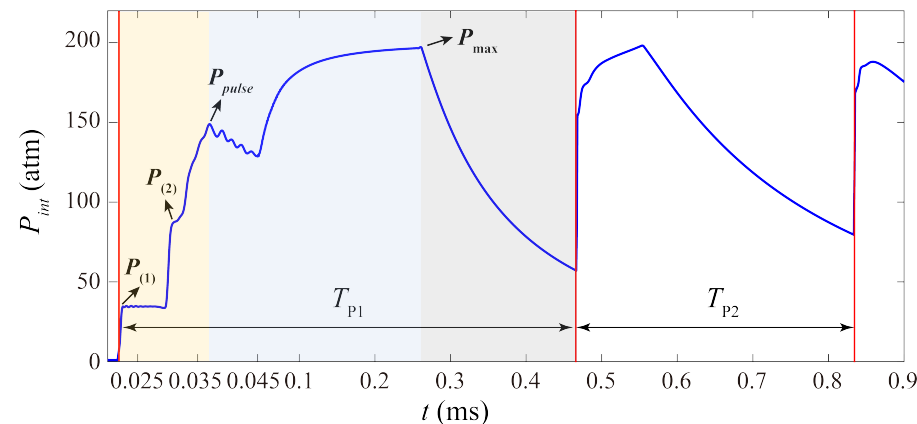
➤ Characteristics of the interface pressure profile

- Case W1: $P_b=200\text{atm}$, $L_b=40\text{mm}$, $\delta=20\text{mm}$



- Periodic oscillations
- Amplitudes decrease and eventually converges

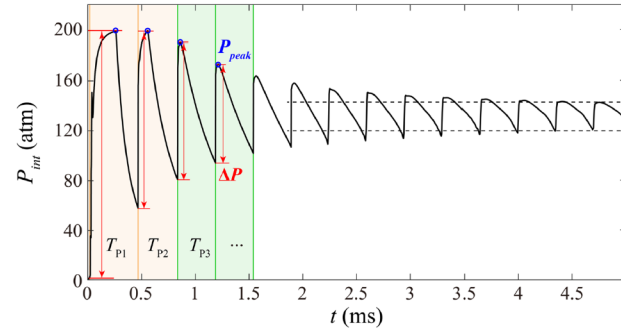
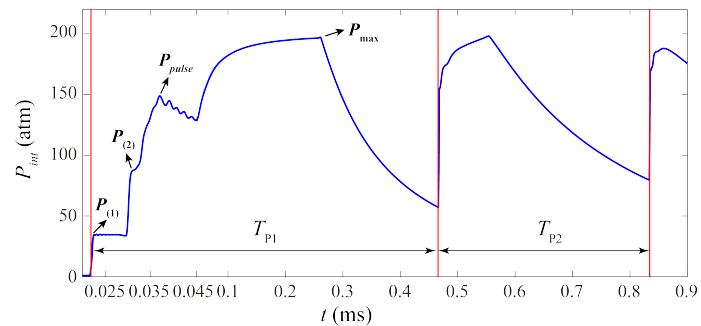
- 1st, 2nd oscillation period (T_{P1}, T_{P2}) :
Pressure **keep rising** after the initial jump
- Subsequent periods (T_{P3}, \dots) :
Pressure **decrease immediately** following each jump



- During T_{P1} : 3 stages
Initial jump — **keep increasing** — **decline**
A step-like profile
- multiple jumps, $P_{(1)}, P_{(2)}$
- reaching a local peak pressure, P_{pulse}

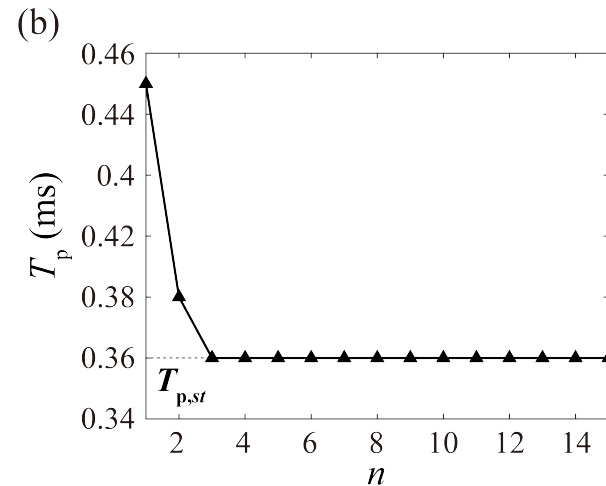
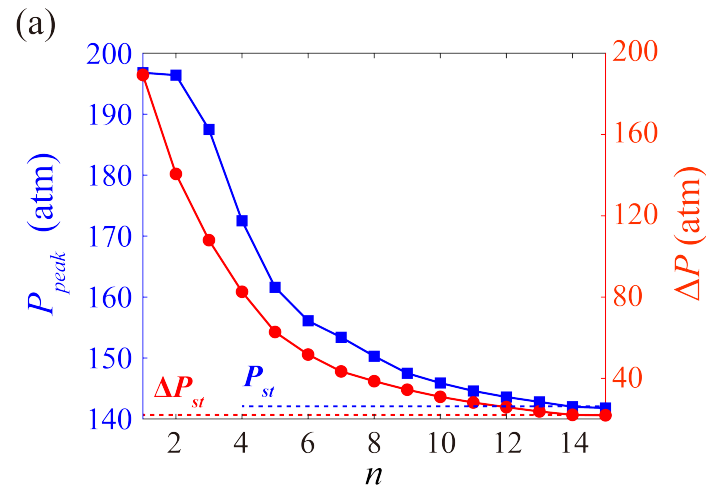
Analysis: Key parameters

➤ Key parameters describing the evolution of **solid** interface pressure



• Short-term behavior

- (1) Primary pulse pressure, P_{pulse}
- (2) The global maximum pressure, P_{max}



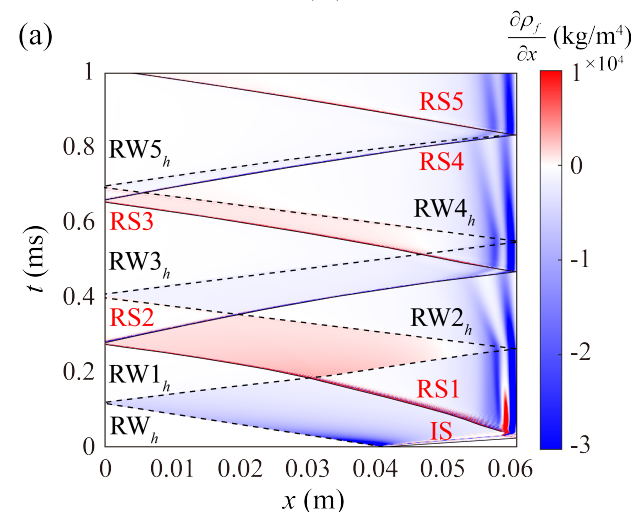
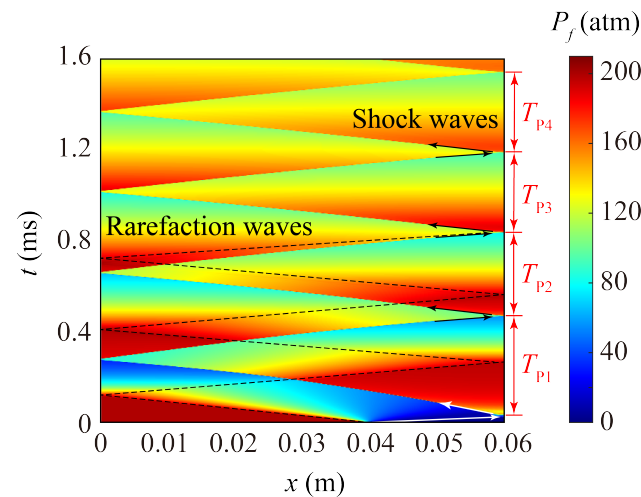
• Long-term behavior

- (3) Oscillation periods to steady state, n_{st}
- (4) The steady-state peak pressure, P_{st}
- (5) The steady-state oscillation amplitude, ΔP_{st}
- (6) The steady-state period duration, $T_{p,st}$

Analysis: Blast loading on **solid** interface

➤ Mechanisms of the pressure evolution

- Case W1: $P_b=200\text{atm}$, $L_b=40\text{mm}$, $\delta=20\text{mm}$

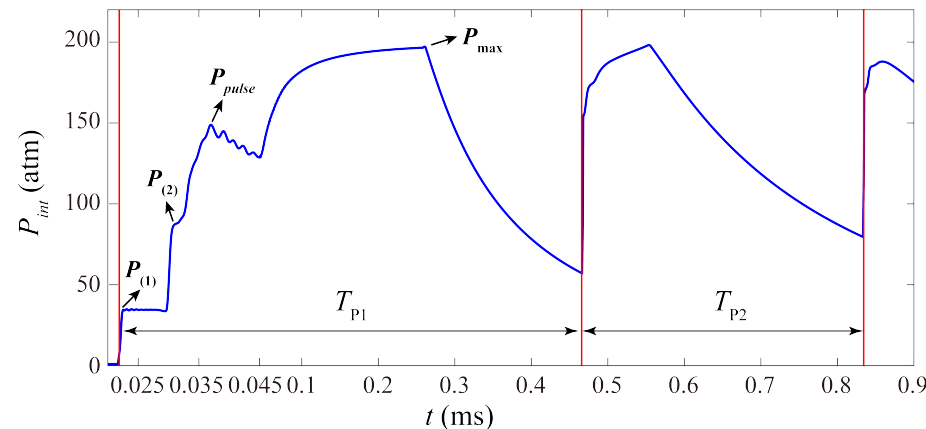
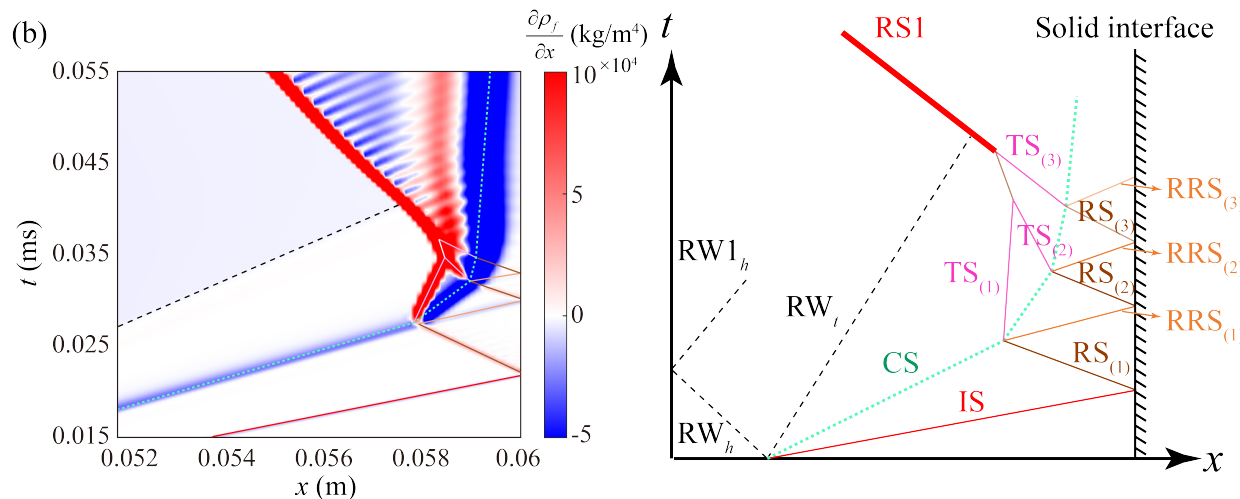


Phenomenon	Reason
Periodic oscillations	Shock/rarefaction waves experience periodic reciprocation due to reflections and repeatedly impact the interface
Amplitudes decrease and eventually converges	The intensities of shock/rarefaction waves gradually weakened
After the 2 nd oscillation period, pressure decrease immediately following each jump	Rarefaction waves catch up and merge with the shock waves during the second period Only a combined wave propagating in the flow field afterwards

Analysis: Blast loading on **solid** interface

➤ Mechanisms of the pressure evolution

- Case W1: $P_b=200\text{atm}$, $L_b=40\text{mm}$, $\delta=20\text{mm}$

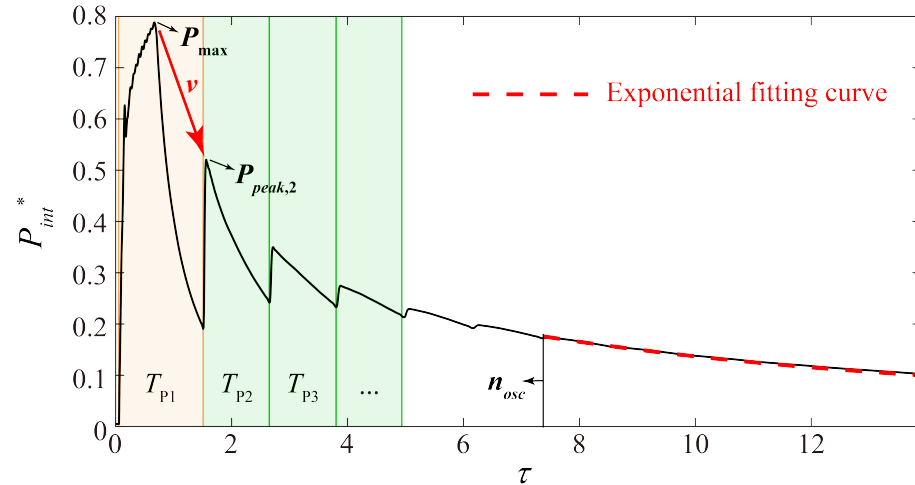


Phenomenon	Reason
A step-like pressure profile	<p>$RS_{(1)}$ reflects repeatedly at the CS and the solid interface</p> <p>Each reflection induce a pressure jump, $P_{(1)}$, $P_{(2)}$</p>
The establishment of the local peak pressure, P_{pulse}	The shock intensity decreases after each reflection
The pressure keeps increasing before reaching the maximum	<p>0.045ms, the rarefaction tail (RW_t) arrives at the interface</p> <p>Internal energy of the fluid at the interface continuously converts into pressure potential</p>

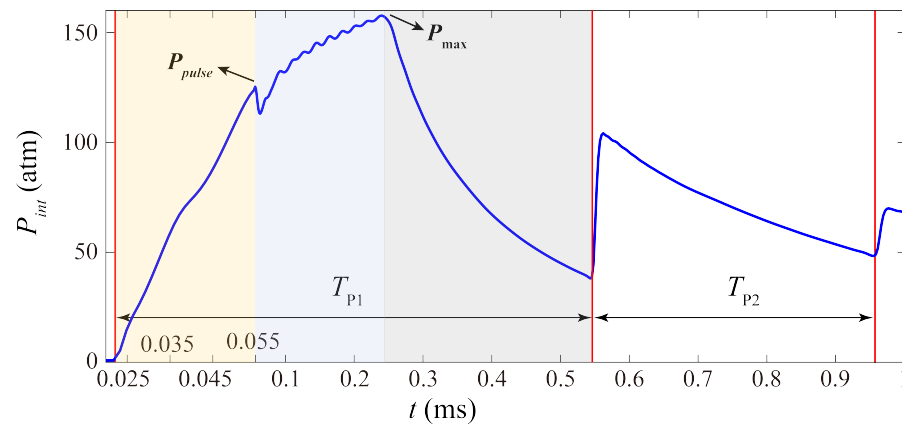
Results: Blast loading on porous interface

➤ Characteristics of the interface pressure profile

- Case P1: $P_b=200\text{atm}$, $L_b=40\text{mm}$, $\delta=20\text{mm}$, $\phi_0=0.65$



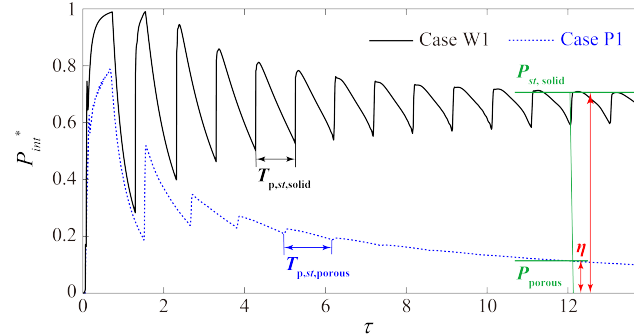
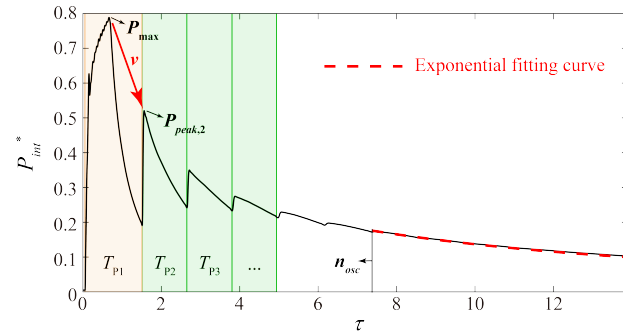
- **Periodic oscillations**
- **Amplitudes decrease rapidly and disappear**
- **During later period — an exponential pressure decay**



- **1st oscillation period (T_{P1}) :**
Initial jump — keep increasing — decline
No step-like pressure jumps
- **Subsequent periods (T_{P2} , ...) :**
Pressure **decrease immediately** following each jump

Analysis: Key parameters

➤ Key parameters describing the evolution of **porous** interface pressure



(1) Primary pulse pressure, P_{pulse}

(2) The global maximum pressure, P_{\max}

(3) The steady-state period duration, $T_{p,st}$

Scaling:

- Nondimensional pressure $P^* = \frac{P - P_1}{P_b - P_1}$

Blast overpressure

- Nondimensional time $\tau = t / T_{p,st,solid}$

Characteristic time

(4) The attenuate rate, ν

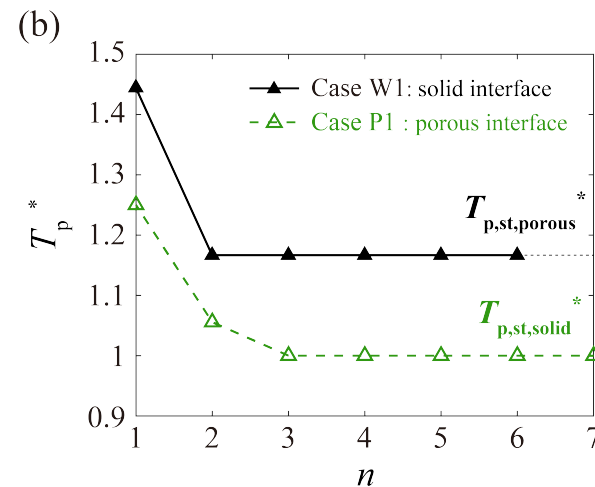
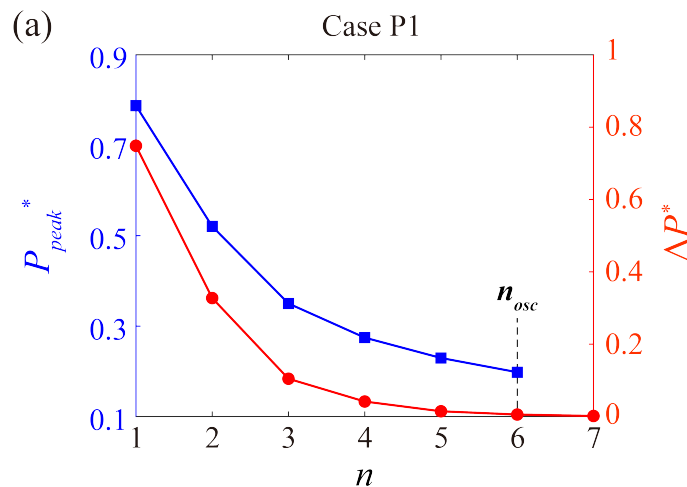
(Measures the speed of pressure decay)

The ratio of the decrease in peak pressure from the first to the second period

(5) The attenuate index, η

(Measures the blast mitigation performance)

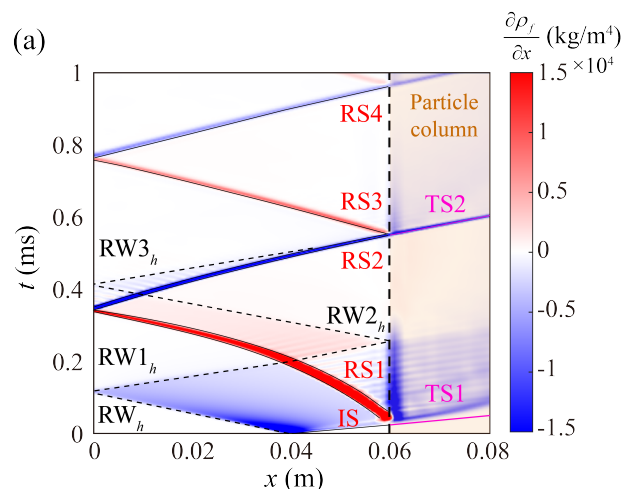
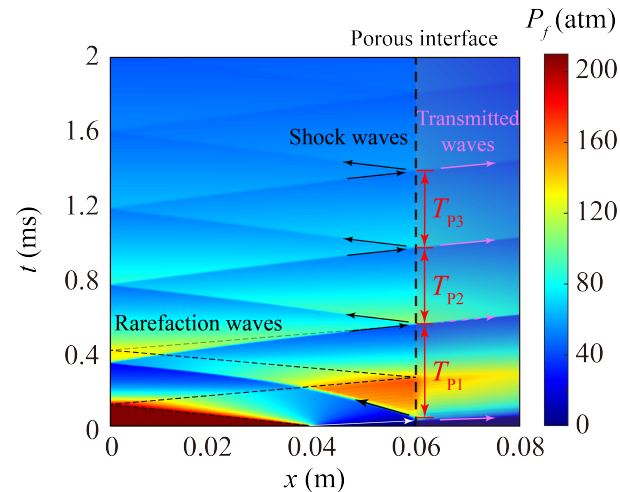
The ratio of interface pressure (porous vs. solid) when the steady peak pressure is reached



Analysis: Blast loading on porous interface

➤ Mechanisms of the pressure evolution

- Case P1: $P_b=200\text{atm}$, $L_b=40\text{mm}$, $\delta=20\text{mm}$, $\phi_0=0.65$

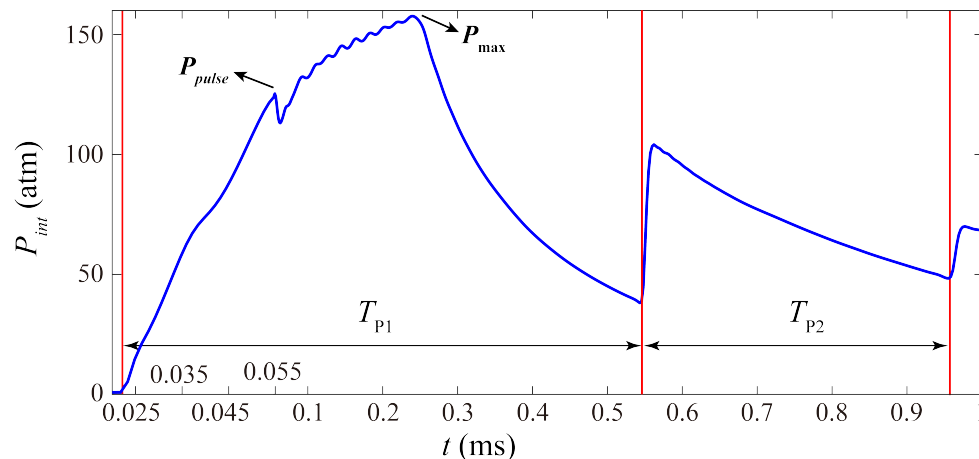
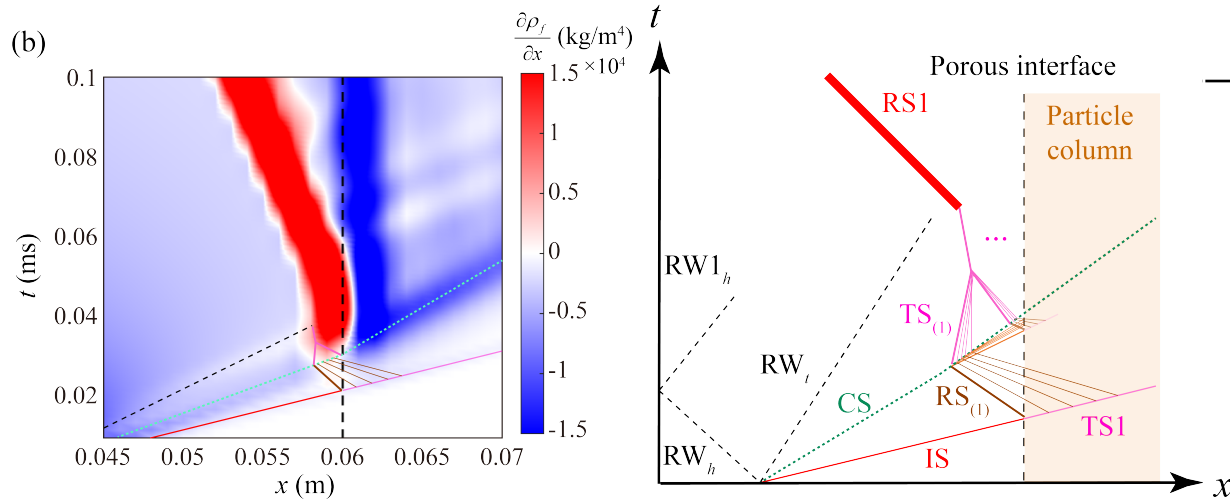


Phenomenon	Reason
Periodic oscillations	<p>Reciprocating shock/rarefaction waves repeatedly impact the interface</p> <ul style="list-style-type: none"> The reciprocating waves partially transmit into the column The fluid gradually infiltrates into the column <p>The intensities of the shock waves quickly attenuates during propagation and soon barely induce a pressure increase</p>
After T_{p1} , pressure decrease immediately following each jump	Rarefaction waves are present only in the first period

Analysis: Blast loading on porous interface

➤ Mechanisms of the pressure evolution

- Case P1: $P_b=200\text{atm}$, $L_b=40\text{mm}$, $\delta=20\text{mm}$, $\phi_0=0.65$

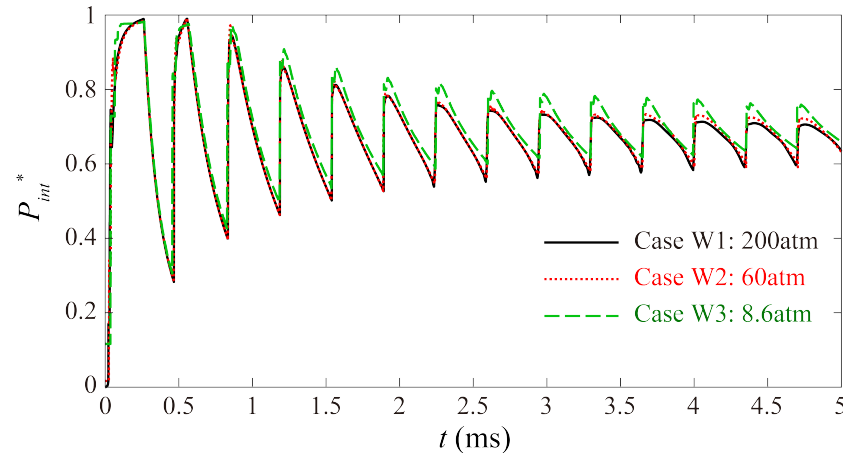


Phenomenon	Reason
<p>No step-like pressure jumps</p> <p>The pressure rise is more smooth</p>	<ul style="list-style-type: none"> The transmitted shock (TS1) reflects off each layer of the column, generating a series of compression waves The CS also propagates into the column <p>The interface pressure is influenced by various waves rather than a single shock</p>
<p>The pressure keeps increasing before reaching the maximum</p>	<p>Internal energy of the fluid at the interface continuously converts into pressure potential</p>

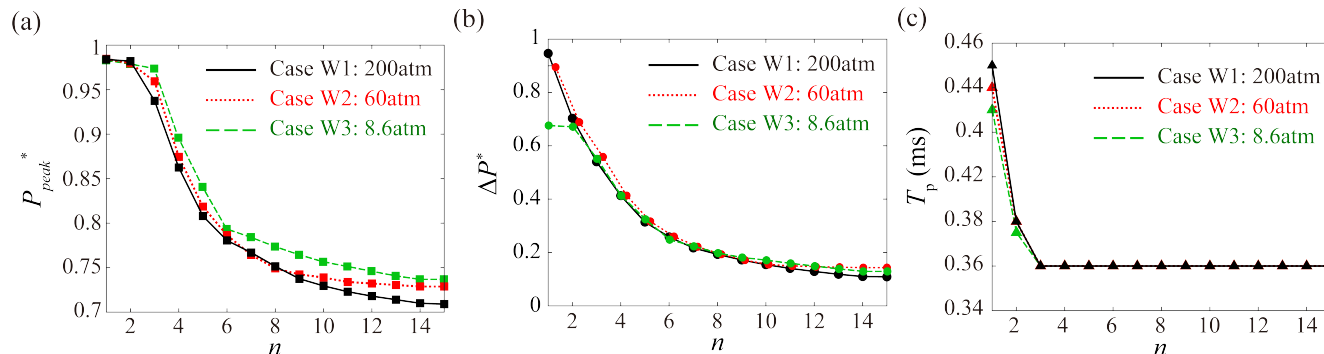
Results: Parameter effects

➤ 1. The blast pressure

• Solid interface



- The interface pressure profiles almost coincide
- Exhibit oscillatory decay with the amplitude eventually stabilize



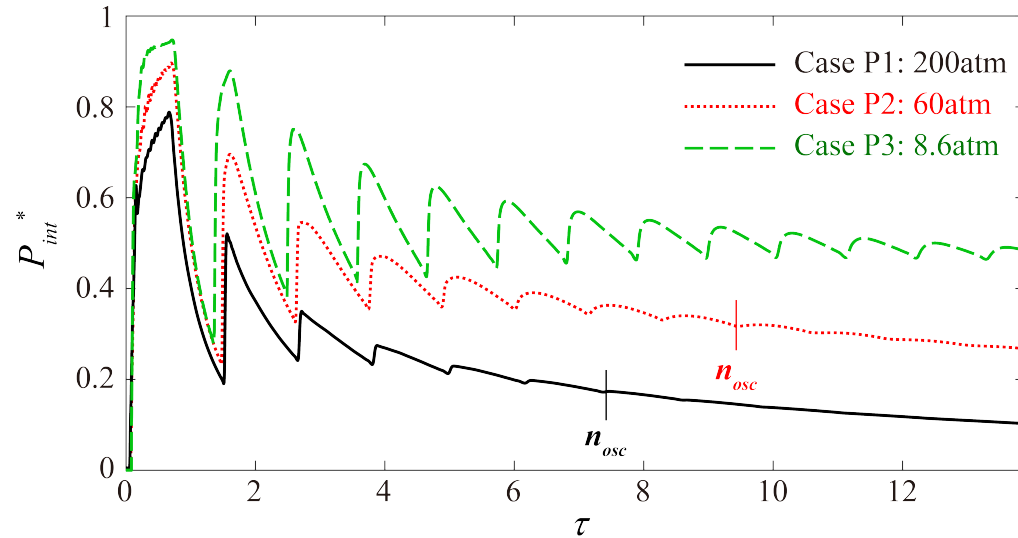
Key Parameters	$P_b=200\text{atm}$	$P_b=60\text{atm}$	$P_b=8.6\text{atm}$
P_{pulse} (atm)	148.6	53.0	8.40
P_{max} (atm)	196.8	59.1	8.47
n_{st}	14	14	14
P_{st}^*	0.71	0.73	0.74
ΔP_{st}^*	0.11	0.14	0.13
$T_{p,st}$ (ms)	0.36	0.36	0.35

Despite the significant differences in blast pressures, the long-term behavior of the interface pressure remains almost identical

Results: Parameter effects

➤ 1. The blast pressure

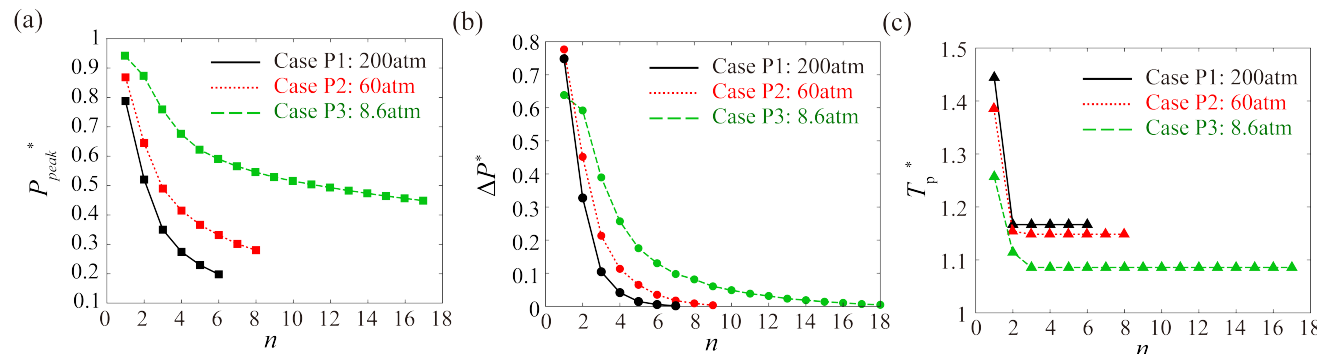
• Porous interface



The oscillation disappears later



Key Parameters	$P_b=200\text{atm}$	$P_b=60\text{atm}$	$P_b=8.6\text{atm}$
$P_{pulse} \text{ (atm)}$	125.3	39.8	5.93
$P_{max} \text{ (atm)}$	157.5	52.1	8.16
$T_{p,st} \text{ (ms)}$	0.42	0.40	0.35



ν

0.34

0.26

0.06

The pressure-driven fluid filtration weakens,
the energy loss in the confined flow field reduces

η

0.15

0.40

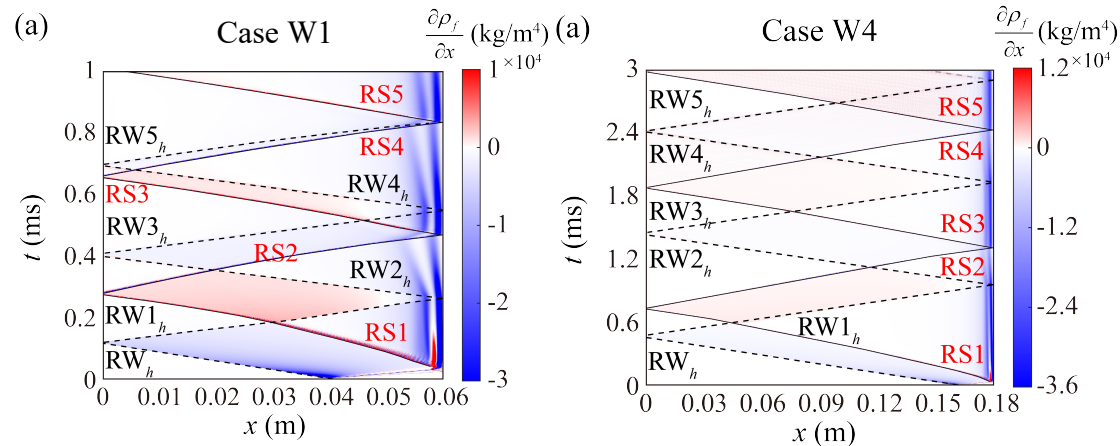
0.73

When subjected to high blast pressures,
a particle column can effectively mitigate the blast

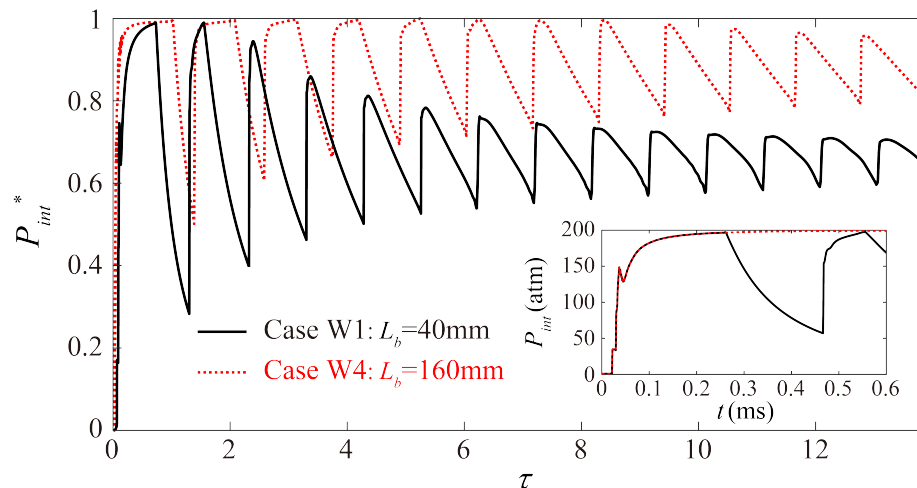
Results: Parameter effects

➤ 2. The volume of blast source (Length of driver section)

• Solid interface



- (Right) The rarefaction waves merge with the shock waves much later

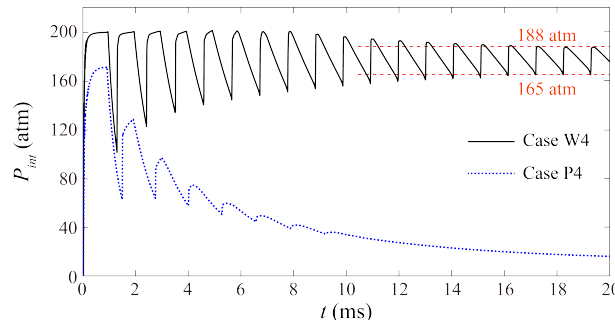
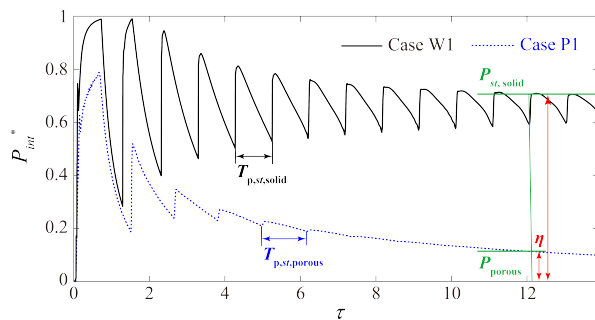
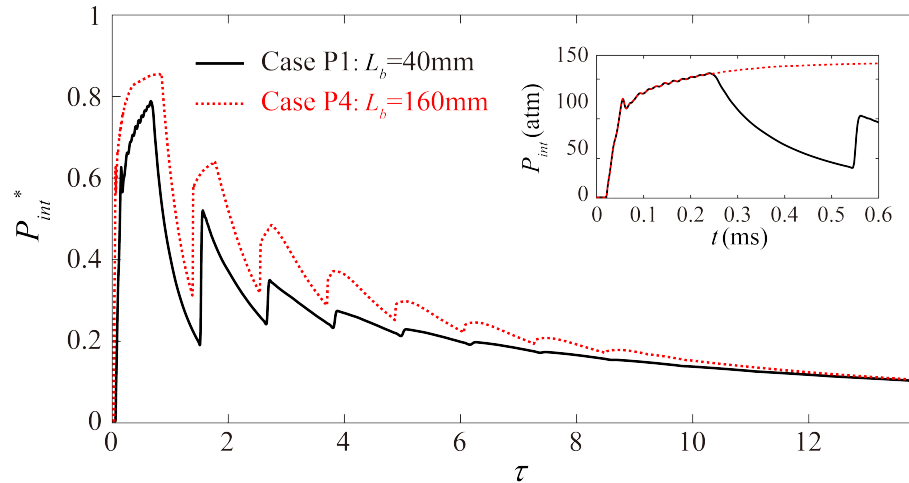


Key Parameters	$L_b=40$ mm	$L_b=160$ mm
P_{pulse} (atm)	148.6	148.6
P_{max} (atm)	196.8	199.6
(Right) RW1h arrives later at the interface, leading to a prolonged pressure increase		
n_{st}	14	17
Increased blast energy, slower pressure decay		
P_{st} (atm)	142	188
The peak pressure takes longer to stabilize and reaches a higher steady value		
ΔP_{st} (atm)	22	23
$T_{p,st}$ (ms)	0.36	1.08
Tripled length of reflection path for the shock waves		

Results: Parameter effects

➤ 2. The volume of blast source (Length of driver section)

• Porous interface



Key Parameters	$L_b=40\text{mm}$	$L_b=160\text{mm}$
P_{pulse} (atm)	125.3	125.3
P_{max} (atm)	157.5	171.3
$T_{p,st}$ (ms)	0.42	1.25

ν

0.34

0.25

The proportion of energy lost through filtration and transmission is smaller relative to the blast energy, leading to a slower decay of the interface pressure

η

0.15

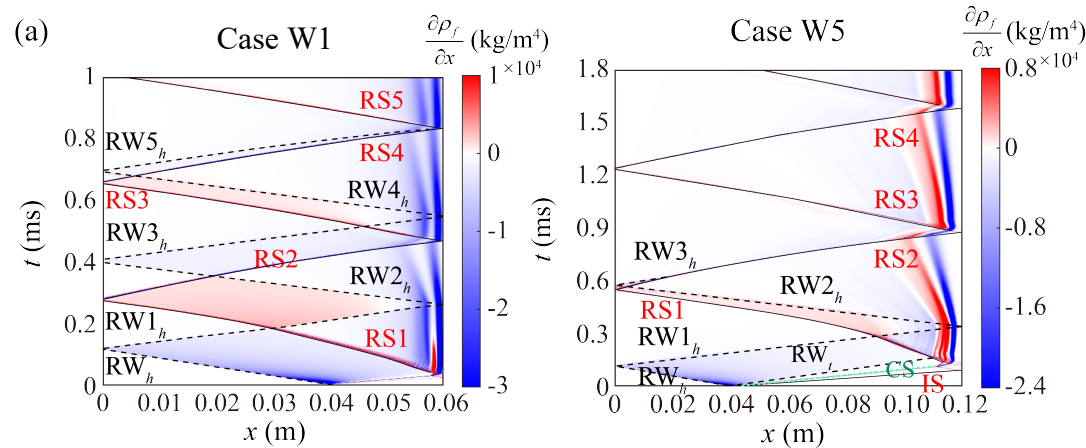
0.098

For higher blast energy, the blast mitigation performance of the same particle column is even better

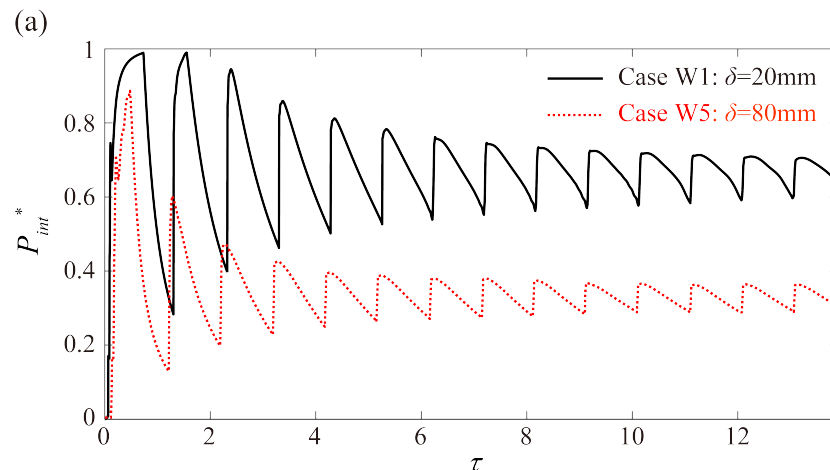
Results: Parameter effects

➤ 3. The stand-off distance

• Solid interface



- (Right) The rarefaction waves merge with the shock waves much earlier



Key Parameters

$\delta=20\text{mm}$

$\delta=80\text{mm}$

P_{pulse} (atm)

148.6

147.6

P_{max} (atm)

196.8

175.3

n_{st}

14

10

P_{st} (atm)

142

73

- (Right) (1) The expansion of the blast air is more significant
- (2) The waves remaining between the CS and the interface is more intense, carrying away more energy

Both factors contribute to a faster pressure decay

ΔP_{st} (atm)

22

22

$T_{p,st}$ (ms)

0.36

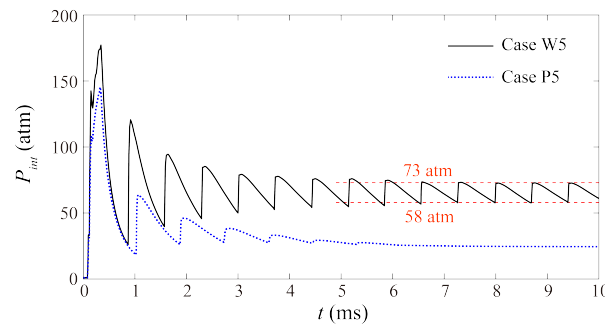
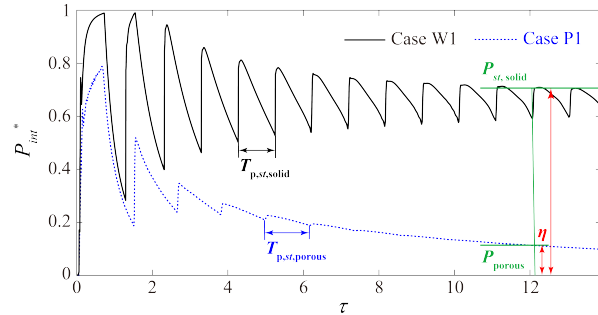
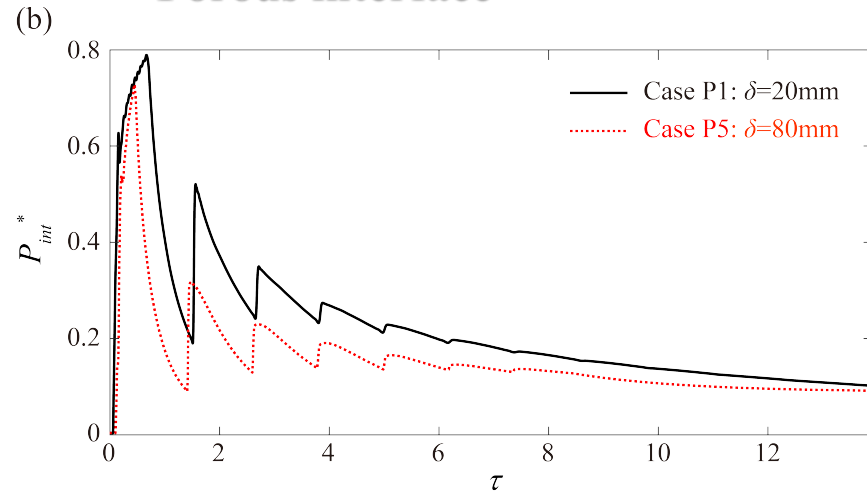
0.71

Doubled length of reflection path for the shock waves

Results: Parameter effects

➤ 3. The stand-off distance

• Porous interface



Key Parameters	$\delta=20\text{mm}$	$\delta=80\text{mm}$
----------------	----------------------	----------------------

P_{pulse} (atm)	125.3	107.8
-------------------	-------	-------

P_{max} (atm)	157.5	145.0
-----------------	-------	-------

$T_{p,st}$ (ms)	0.42	0.85
-----------------	------	------

v

0.34

0.56

(Right) The stronger expansion of the blast air leads to a faster pressure decay

η

0.15

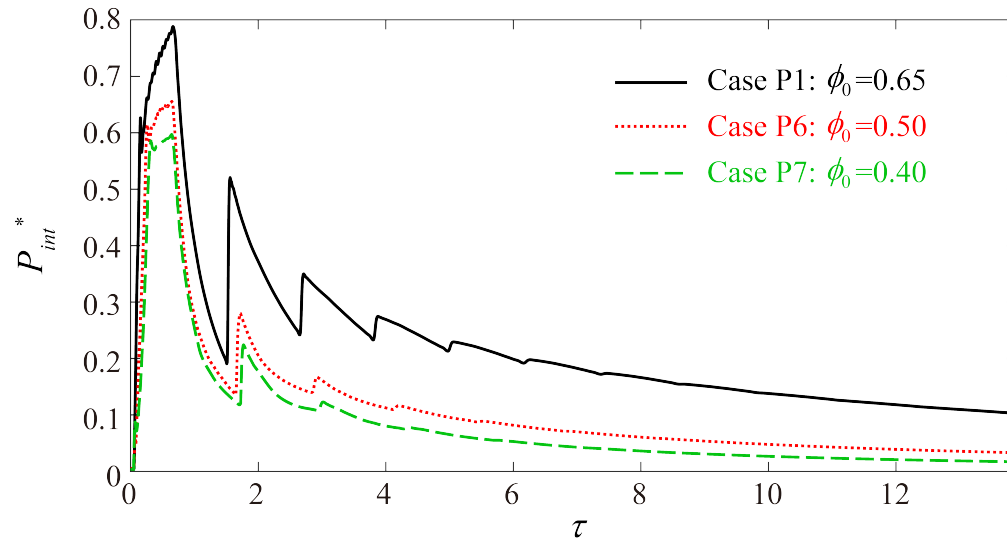
0.35

The fluid expansion has significantly reduced the pressure, making the effects of wave transmission and flow filtration less impactful

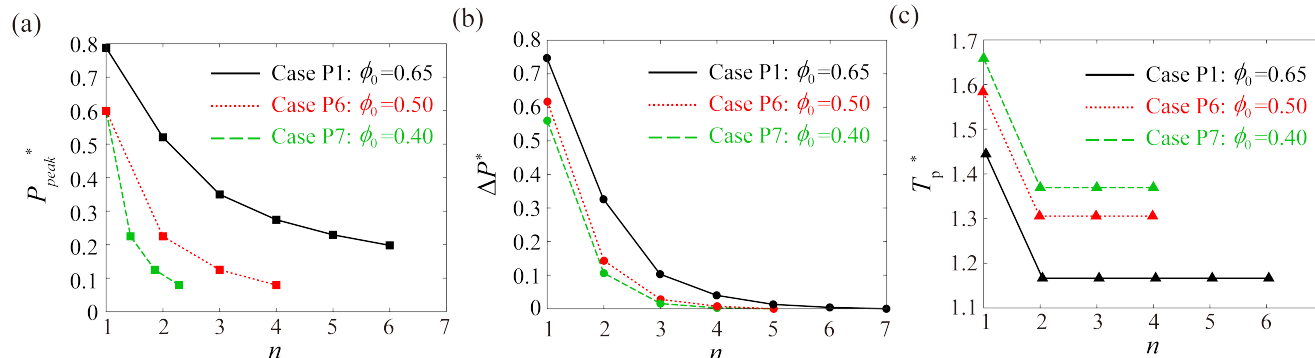
The blast mitigation performance weakens as the distance from blast source increases

Results: Parameter effects

➤ 4. The particle volume fraction



- With increasing volume fraction, the pressure oscillation disappears earlier



Key Parameters	$\phi_0=0.65$	$\phi_0=0.5$	$\phi_0=0.4$
P_{pulse} (atm)	125.3	122.1	117.6
P_{max} (atm)	157.5	131.1	119.8
$T_{p,st}$ (ms)	0.42	0.47	0.49

ν 0.34 0.57 0.62

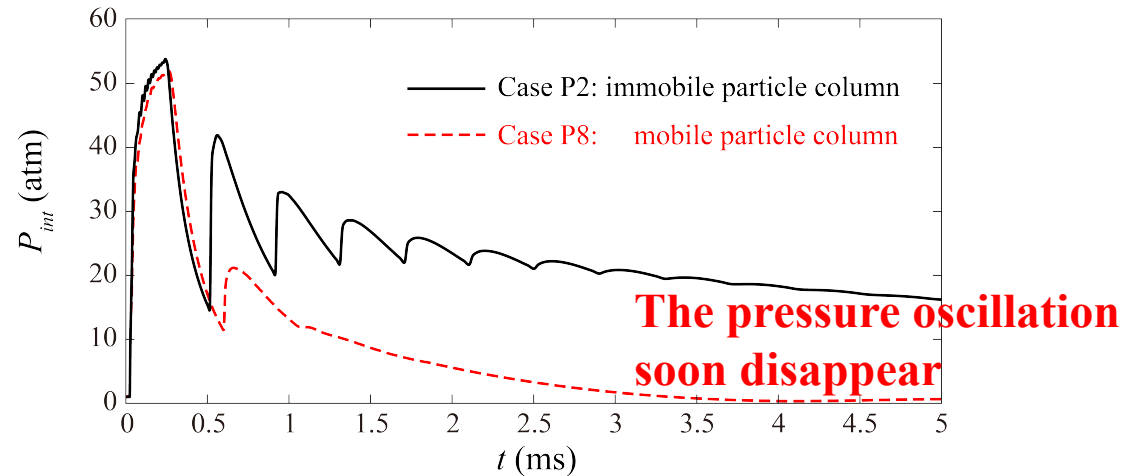
Higher permeability of the column
Stronger wave transmission and fluid filtration
More energy loss of the confined flow field

η 0.15 0.06 0.027

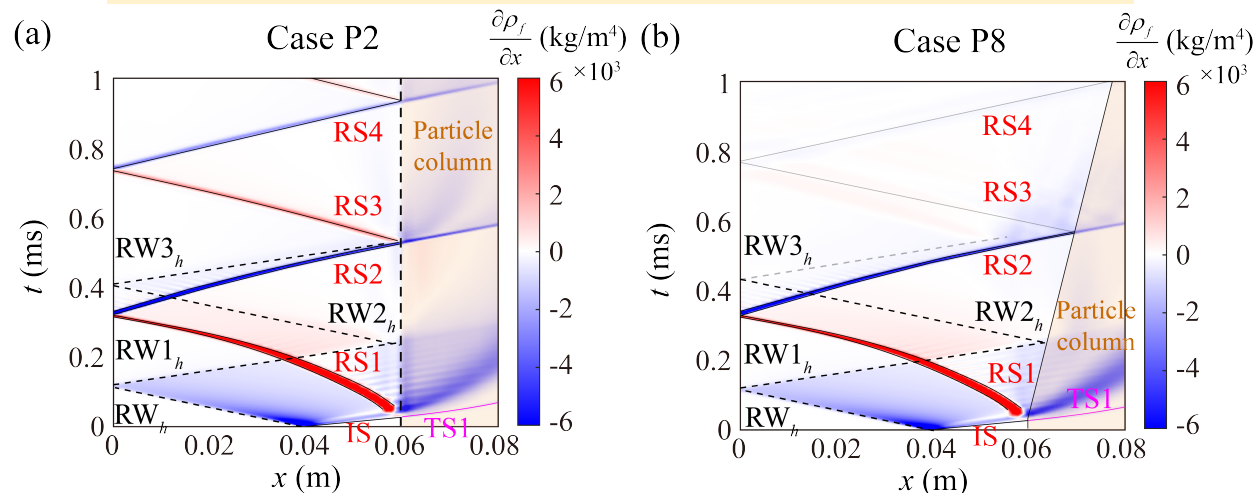
Better blast mitigation performance

Results: Parameter effects

➤ 5. The coupling effect of particle motion



- Before 0.5ms, the pressure profile is similar, since the movement of the interface is limited



Key Parameters	immobile	mobile
P_{pulse} (atm)	39.8	34.5
P_{max} (atm)	52.1	47.9
$T_{p,st}$ (ms)	0.40	—

ν 0.26 0.59

(1) Part of the flow energy is converted into the kinetic energy of the particles

(2) The confined gas expands due to the motion of interface

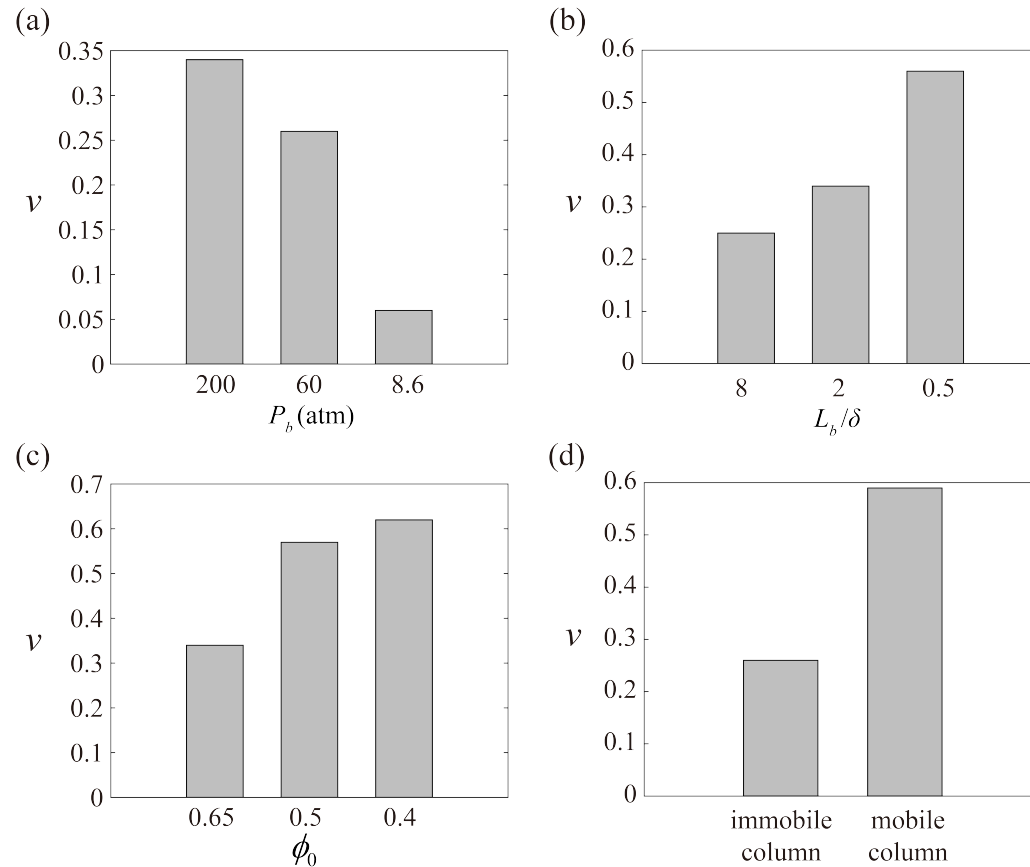
η 0.40 0.022

Significant pressure decay due to particle motion

Discussion

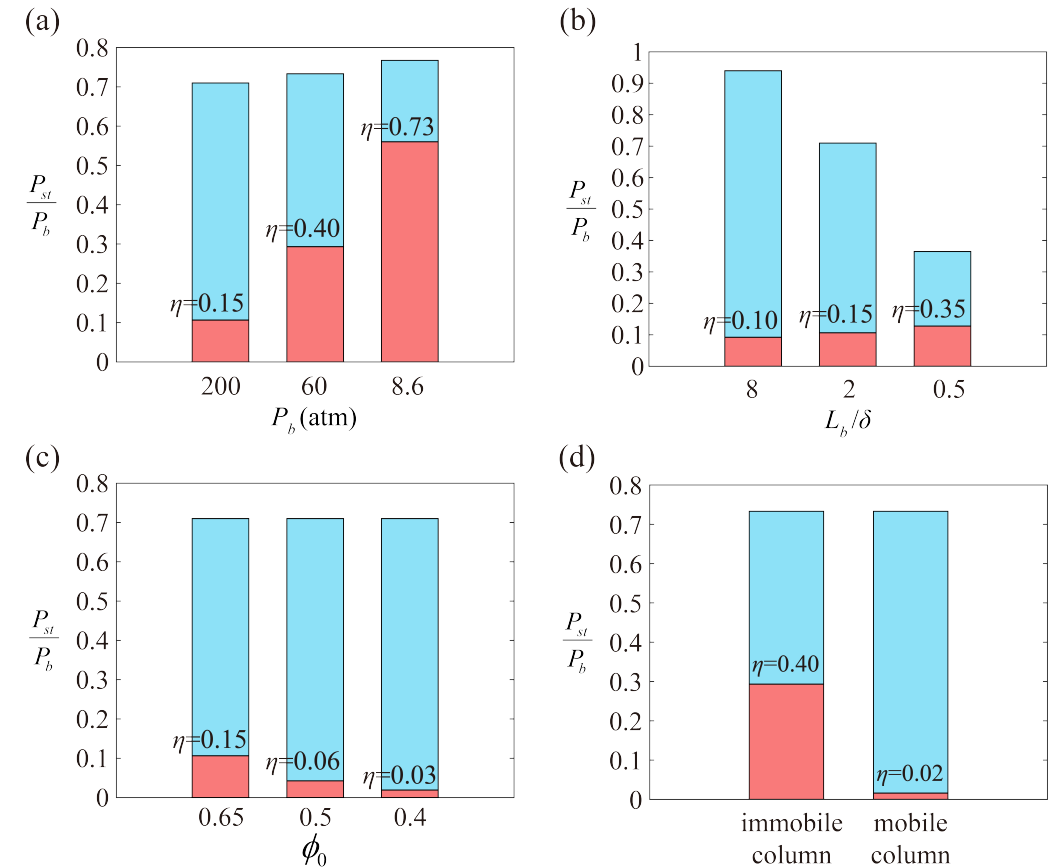
➤ The attenuation rates (ν)

A greater ν represents a faster pressure decay



➤ The attenuation index (η)

A smaller η represents better blast mitigation performance



Conclusion

- **The characteristics of the interface pressure are given**
- **The mechanisms of the pressure evolution are revealed through detailed analysis of wave dynamics**
- **The attenuation rate (ν) and the attenuation index (η) are used to assess the blast mitigation performance of the porous medium**
- **The dependence of these defining features on different loading conditions is revealed**

Thanks for your listening !